



## OVERVIEW OF THE E-ELT MCAO MODULE PROJECT

Emiliano Diolaiti<sup>1,a</sup>, on behalf of the MAORY Instrument Team

<sup>1</sup>INAF Osservatorio Astronomico di Bologna, via Ranzani 1, 40127 Bologna, Italy

**Abstract.** The phase A conceptual design of the Multi-Conjugate Adaptive Optics module for the European Extremely Large Telescope has been developed to provide uniform adaptive optics compensation over an extended field of view in the near infrared with high sky coverage. The module design is based on the use of laser and natural guide stars and multiple deformable mirrors. An overview of the phase A design is given. The ongoing technical activities in preparation for the project phase B are described.

### 1. Introduction

MAORY is the Multi-Conjugate Adaptive Optics (MCAO) module for the European Extremely Large Telescope (E-ELT [1]). The phase A of the MAORY project was completed in December 2009 in the framework of the preliminary studies of the E-ELT instrumentation [2] sponsored by the European Southern Observatory (ESO). The MCAO module is now included in the telescope's first light instrumentation set. The MCAO module phase A design [3] has been optimized to fulfill the requirements of the E-ELT high angular resolution camera MICADO [4], keeping a provision to feed other scientific instruments through an additional exit port. At the moment of this writing the project activities are focused on one side on the project organization and on the other side on the review of the scientific requirements and of the technical solutions in collaboration with ESO. This paper gives an overview of the phase A design and describes the current activities and developments in preparation for the next project phases.

### 2. MCAO module phase A design

#### 2.1. General overview

The MCAO module has to relay the telescope focal plane to the science instruments and to compensate the disturbances affecting the incoming optical wavefront, mainly due to atmospheric turbulence and telescope windshake. A functional block diagram of the MCAO module is shown in the next figure. Light comes in from the E-ELT focal plane and is propagated through the common path optics and the post-focal Deformable Mirrors (DM) inside the MCAO module. A dichroic beam-splitter splits the science and the Laser Guide Stars (LGS) beams. The science beam propagates through the science path

---

a e-mail : emiliano.diolaiti@oabo.inaf.it

optics to the exit focal plane, where the outer part of the field is selected by the Natural Guide Star (NGS) Wavefront Sensor (WFS), while the central part of the field is reserved for the science instrument. The LGSs beams propagate through the LGS objective and enter the LGS WFS. The signals from the LGS and the NGS WFS are used by the real time control system to compute commands for the DMs inside the MCAO module and for the adaptive and tip-tilt mirrors in the telescope, controlled by the telescope control system. All the MCAO module operations are supervised by the instrumentation software, which also interacts with the telescope control system and with the client instrument instrumentation software.

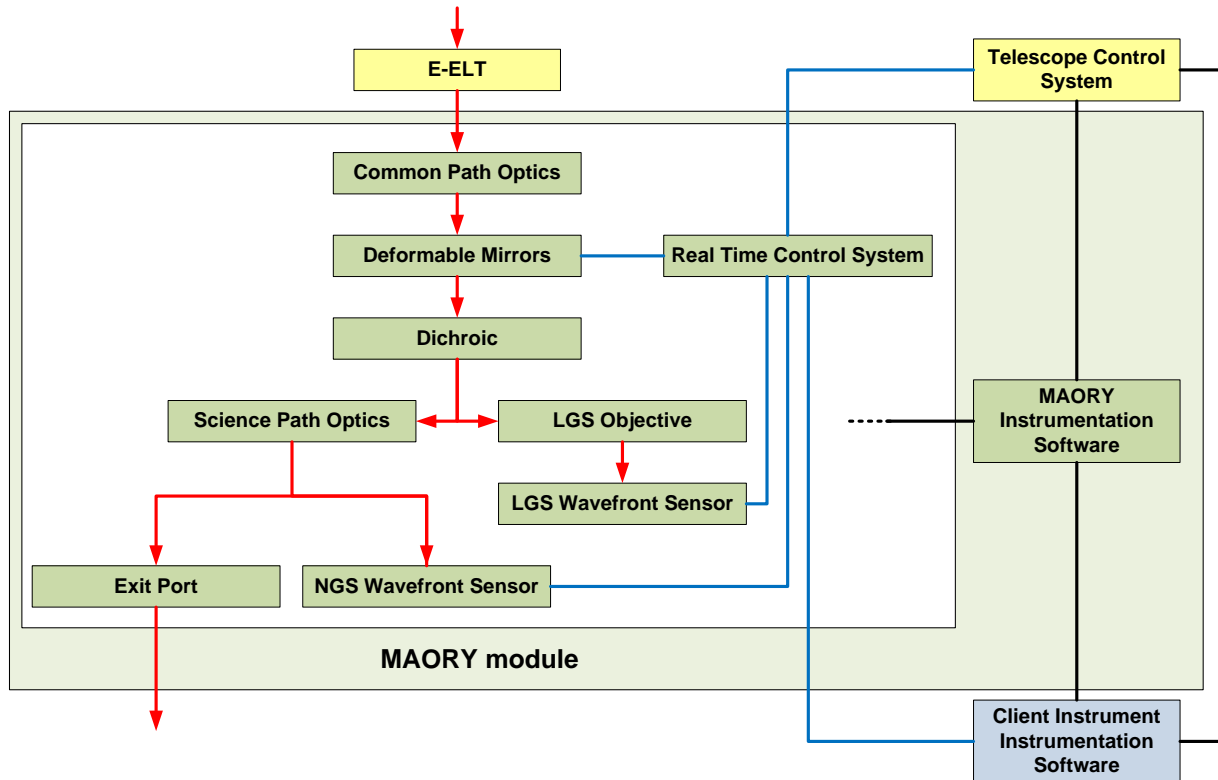


Fig. 1. MCAO module functional block diagram. Red arrows indicate the light path. Blue and black lines represent data/signal links (blue: real time; black: non real time). The links between the MAORY instrumentation software and the MAORY sub-systems are not shown for simplicity.

From the optical design point of view, the MCAO module is a finite conjugate relay formed by two pairs of aspheric off-axis mirror. Flat fold mirrors (two of which are deformable) allow to fit the module into the allocated area on the Nasmyth platform. The output focus has the same focal ratio and exit pupil location as the telescope direct focus. The only notable difference in the optical interface is the rather strong field curvature on the output focus. The splitting of the science and LGS beams in the optical relay is accomplished by means of a dichroic beam-splitter, which transmits the LGS light; the science channel path is fully reflective. The LGS beams transmitted by the dichroic beam-splitter are collected by a refractive objective which creates the LGS images; refocusing is required to compensate for the sodium range variation with zenith distance. The module feeds two focal stations: a gravity invariant port for MICADO with mechanical field derotation and a lateral port for other scientific instruments detached from the module.

## 2.2. Adaptive optics and operational concept

The client instrument MICADO requires uniform adaptive optics compensation over a scientific field of view of  $53 \times 53$  arcsec<sup>2</sup> on the wavelength range 0.8-2.4  $\mu$ m.

In order to ensure this performance, the adaptive optics system of MAORY is based on the use of proven and robust techniques, also adopted in the design of the Thirty Meter Telescope's NFIRAOS module [5]. MCAO, originally proposed by Beckers [6], has been proven on sky by MAD on VLT [7] and by GeMS on Gemini [8, 9] and is adopted in the case of MAORY to ensure performance uniformity and high sky coverage. Laser Guide Stars (LGSs) have been proven on sky in several cases and in particular together with MCAO by GeMS itself. Finally the wavefront sensors within MAORY are placed downstream the DMs in the light path to ensure optical feed-back.

Wavefront errors compensation is performed by the MCAO module driving the telescope's adaptive mirror M4 and tip-tilt mirror M5 and by two post-focal DMs integrated in the MCAO module itself and conjugated to high altitude turbulent layers at 4 km and 12.7 km. The requirement for the DMs inter-actuator spacing is that the projected pitch onto the layer has to be 1 m.

Wavefront sensing is performed by a LGS WFS using 6 sodium artificial sources, which are arranged on a circle of 2 arcmin angular diameter. The LGS WFS is complemented by a NGS WFS using 3 natural stars which can be searched inside an annular field of 2.6 arcmin diameter, the central part of which is reserved for the science instrument. The NGS WFS is devoted to the measurement of the orders of wavefront aberration that the LGS WFS alone cannot measure in a reliable way. As a baseline, in each of the 3 NGS WFS channels, the infrared light of wavelength 1.5-1.8  $\mu\text{m}$  is used to measure fast tip-tilt and focus. The adopted wavelength range allows to greatly increase sky coverage, thanks to the spot shrinking ensured by MCAO: stars as faint as magnitude  $H = 21-22$  can be used. The light of wavelength 0.6-0.9  $\mu\text{m}$  is sent to a so-called Reference WFS, which is operated at low temporal frequencies and relatively low pupil sampling (in the order of  $10 \times 10$  subapertures) to monitor the LGS non-common path aberrations related to the sodium layer profile variability [10] coupled with field truncation and other instrumental effects in the LGS WFS.

The LGS constellation is kept fixed with respect to the telescope pupil and thus, seen from the E-ELT Nasmyth platform, it rotates with the elevation axis. The LGS WFS and the post-focal DMs are rotated at the same rate. In this way the LGS WFS and all DMs (post-focal and telescope M4/M5) are reciprocally fixed. This property allows to relax the requirement on the update rate of the control matrix in the real-time computer, since the only residual variation is the diameter of the LGS footprints, projected on the high-altitude layers, that however implies a very slow control matrix update rate. An alternative strategy is to avoid rotating the post-focal DMs: the wavefront correction is computed on "virtual" DMs and then rotated onto the actual ones. This strategy simplifies the opto-mechanics and has to be further investigated, in particular concerning the calibration aspects.

According to preliminary calculations carried out in the project phase A, the MCAO module expected performance is 50% Strehl Ratio averaged over the MICADO field of view at 2.16  $\mu\text{m}$  wavelength with 50% sky coverage at the Galactic Pole. Accepting a slight Strehl Ratio degradation to 40%, sky coverage at the Galactic Pole increases to 80%.

### **3. Preparing for the phase B of the project**

#### **3.1. Developments related to the adaptive optics system**

A significant effort is devoted to the development of a laboratory prototype to emulate the wavefront sensing system of the E-ELT MCAO module. This prototype, including a  $40 \times 40$  subapertures Shack-Hartmann WFS, was designed and built a few years ago [11, 12] to reproduce elongated LGS spots similar to those expected for the E-ELT. The prototype design has been recently upgraded to include the possibility to emulate multiple sources, dynamic turbulence and to generate arbitrary sodium

profiles through a remotely controllable spatial light modulator. At the moment of this writing, the refurbished prototype is under integration and verification. Used together with an end-to-end adaptive optics simulation code which is also under development, this prototype will be a very useful tool to support the design of the MCAO system.

Laboratory verification of the adaptive optics performance will be essential for the E-ELT MCAO module. A simplified test would be to inject wavefront distortions by means of the DMs themselves and testing the capability of the MCAO module to compensate for the disturbance. In order to have a deeper and more robust performance characterization, an external turbulence simulator reproducing the E-ELT optical interfaces at the module entrance would be preferable. In the case of the E-ELT MCAO module, the design of such a turbulence simulator is very complex. A “monolithic” design would require at least 1 meter class optics and a very long optical train. For this reason a “segmented” design is under study, including both LGS and NGS sources and multiple layer dynamic turbulence. The telescope adaptive and tip-tilt mirrors M4 and M5 would be emulated at software level. The status of this activity is reported elsewhere in this Conference [13].

Crucial technology developments, of high relevance for the MCAO module project, are carried out by ESO in collaboration with other organisations as reported elsewhere in this Conference [14]: these development activities are concerned with large format detectors and cameras for LGS wavefront sensing, DM technologies, real-time control platforms.

### **3.2. Post-focal relay optical design**

After the project phase A the post-focal relay optical design has been significantly reviewed to solve issues such as the field curvature of the output focal surface and to mitigate technological risks.

A trade-off study has been started to investigate the impact of different DM technologies [15] on the optical design. The required projected pitch of the post-focal DMs actuators on the atmospheric layers is in the order of 1 m, corresponding to about 40-50 actuators across the DM diameter. Depending on the physical inter-actuator distance, this requirement also sets the required diameter of the pupil image produced by the post-focal relay and the diameter of the DMs. Three different cases have been considered: “small” DMs ( $\approx 150$  mm diameter), “medium” DMs ( $\approx 300$ -500 mm diameter), “large” DMs ( $\approx 1000$ -1300 mm diameter). The first class has been considered at a very preliminary level only because, as discussed in the following, it does not seem suited to the E-ELT MCAO module. Preliminary designs for the other two classes have been developed to assess their feasibility and compatibility with the E-ELT requirements and interfaces. The medium and large class DMs could be based respectively on piezo-electric [16] and voice coil motor [17] actuator technology.

A small DM implies a very large pupil de-magnification factor, which corresponds to a large longitudinal de-magnification, increasing quadratically with lateral de-magnification, so that the distance between the planes conjugated to the 12.7 km and 4 km layers in image space is smaller than the deformable mirror diameter. Therefore an intermediate re-imaging between the two DMs is necessary requiring a complex design. The second consequence of the large pupil de-magnification is that the rays are very skew and a given tilt of the deformable mirror with respect to the optical axis corresponds to a large tilt of the deformable mirror conjugate plane in object space with respect to the atmospheric layer. A third aspect is that in order to achieve the required optical performance (diffraction-limited wavefront error) it is necessary to adopt complex optical schemes with many elements, reducing throughput and increasing thermal emissivity. A small DM also requires a “fast” collimator. A design of this sub-system has been attempted (figure 2), based on a primary mirror with prime focus corrector, which is a configuration that usually gives fast focal ratios. The mirror and the

prime focus corrector are off-axis; the lenses are aspherical. The difficulty in achieving the required wavefront error with this design confirms the previous analysis.

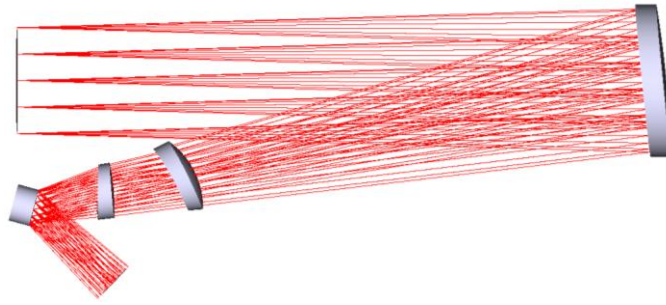


Fig. 2. Collimating optics to match the pupil image to a 150 mm diameter deformable mirror (shown on the left).

The optical designs for medium and large DMs are based on the optical scheme shown in figure 3, with suitable adaptations: a concave off-axis mirror creates a pupil image of size depending on the focal length of the mirror itself, and a 3-mirror system (concave – convex - concave) re-images the entrance focal surface to the exit port. The DMs and the dichroic beam-splitter to separate science and LGS beams can be placed close to the intermediate pupil image. By suitable optimization this design can be modified to achieve different pupil image size, while keeping on the exit port the same optical interface as on the entrance one (telescope focal surface).

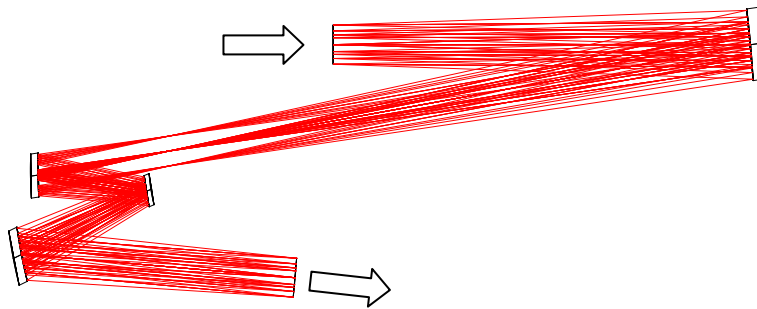


Fig. 3. Post-focal relay optical design, unfolded version. Arrows indicate the light path.

A folded version of this design for medium DMs with inter-actuator spacing of 10 mm is shown in figure 4. The gravity invariant exit port is inside the plane of the figure; the optical axis on the lateral exit port is at  $90^\circ$  with respect to the entrance optical axis, as required by the phase A top level requirements. Switching from the gravity invariant to the lateral exit port is possible by inserting a flat mirror in the beam. The LGS beam after the dichroic beam-splitter is focused by a refractive objective made of 4 lenses, with internal refocusing to track the sodium layer during observations. Just before the final LGS image plane, a flat mirror folds the beam upwards to create a gravity invariant exit port for the LGS WFS sub-system.

The optical performance of this design is good (32 nm RMS wavefront error averaged over the MICADO science field of view). As a consequence of the tilt of the DMs with respect to the atmospheric layer images, the DMs conjugates in object space are between 3.5 and 4.5 km and between 12.2 and 13.2 km respectively: these conjugation ranges have to be compared to the nominal ones, i.e. 4 km and 12.7 km respectively. The maximum RMS blur of the layer images on the two DMs is about  $1/6$  inter-actuator spacing, which seems still acceptable even though larger than the usual rule-of-thumb of  $1/10$  spacing.

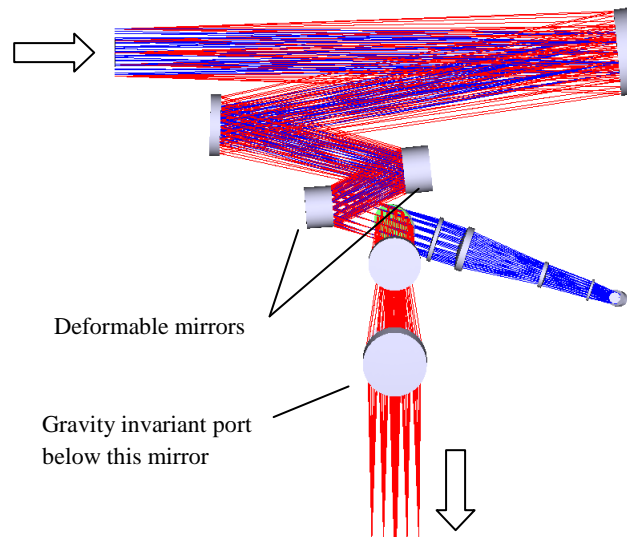


Fig. 4. Post-focal relay (DMs diameter about 500 mm). Red/blue rays: science/LGS path.

Reducing the inter-actuator spacing from 10 to 7 mm significantly degrades the performance. In particular the DM conjugation mismatch increases considerably: the DMs conjugates in object space are between 2.5 and 5.5 km and between 11.1 and 14.3 km respectively, as compared to the nominal ranges of 4 km and 12.7 km. The maximum RMS blur of the layer images on the DMs is about 1/2 inter-actuator spacing. Moreover, due to the more compact size of the post-focal relay, it is more difficult to accommodate the exit ports due to clearance reasons.

The post-focal relay design shown in figure 3 has also been modified for large DMs. The folded version of a possible design for large DMs is shown in figure 5.

The DMs are below the plane of the MAORY bench: this choice allows to exploit the volume below the bench reducing the width. Switching from the gravity invariant to the lateral exit port is possible either by inserting a flat mirror (as shown in figure 5) or by tilting the down-facing mirror that creates the gravity invariant port. The LGS beam after the dichroic beam-splitter is more than 1 m in diameter: the LGS objective consists of a focusing mirror that reduces the beam diameter, followed by a 4-lens group close to its prime focus; the whole assembly is folded by a flat mirror to avoid obscuration effects. Sodium layer tracking is achieved by focusing the lenses close to the prime focus of the mirror.

The optical performance of this design is good (9 nm RMS wavefront error averaged over the MICADO science field of view). The mismatch of the DMs conjugates with respect to the atmospheric layers is significantly reduced with respect to the designs for medium DMs: the DMs conjugates in object space are between 3.8 and 4.2 km and between 12.6 and 12.8 km respectively, to be compared with the nominal ranges of 4 km and 12.7 km respectively. The maximum RMS blur of the layer images on the two DMs is well below 1/10 inter-actuator spacing.

The main conclusions from this preliminary trade-off study focused on the geometrical properties of the DMs can be summarized as follows.

In the medium DMs case, a 10 mm inter-actuator spacing seems to be better than a smaller spacing of e.g. 7 mm because of the layer re-imaging performance, while the overall size of the MCAO module is still within the constraints set in phase A even with 10 mm spacing.

The large DMs design shown in figure 5 is compatible with existing DMs: the DM size and inter-actuator spacing are comparable to the values of the VLT adaptive secondary mirror [17]. The MCAO module in the large DMs case is slightly longer than the phase A design described in section 2.1, while

it is similar in width and lower in height, at the expense of one flat mirror more on the gravity invariant port path. The size of the rigid mirrors is similar to the phase A design. The dichroic beam-splitter is about 1.2 m in diameter, a quite large value, although probably still manageable. Alternative strategies for LGS/science beam splitting are under investigation. Other designs of this class under study, with different layouts, are not shown here for simplicity.

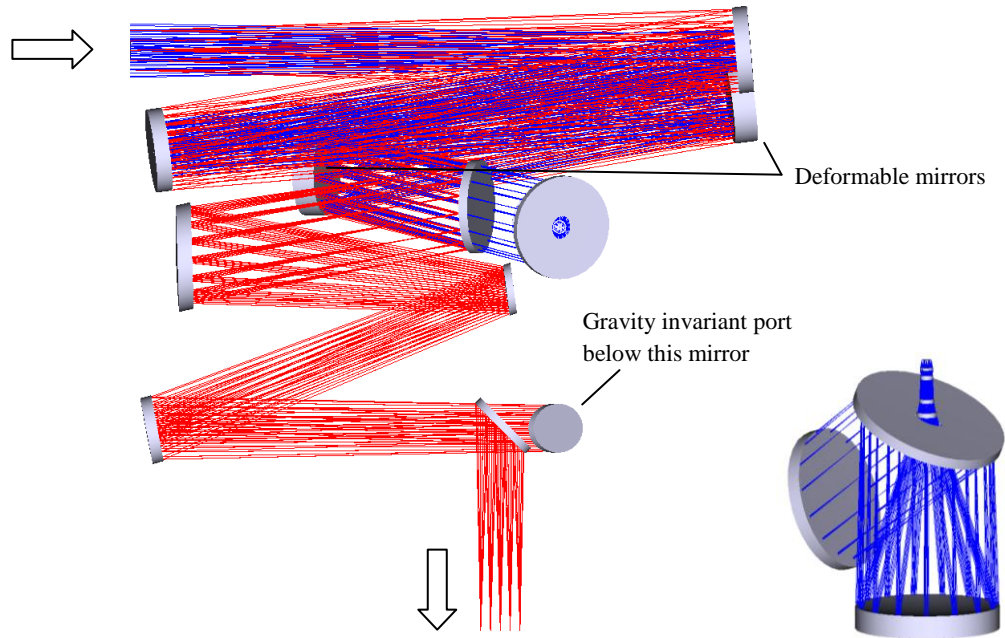


Fig. 5. Left. Post-focal relay design. The DMs in this design are placed below the plane of the figure and have a diameter of about 1100-1200 mm. Right. LGS imaging optics (not to scale). Red/blue rays: science/LGS path.

#### 4. Acknowledgements

This work has been partly supported by the Italian Ministero dell'Istruzione, dell'Università e della Ricerca (Progetto Premiale E-ELT 2012 – ref. Monica Tosi).

#### 5. References

1. R. Gilmozzi, J. Spyromilio, *Proceedings of the SPIE Volume 7012*, ed. L. M. Stepp, R. Gilmozzi, pp. 701219 (2008)
2. S. Ramsay, S. D'Odorico, M. Casali et al., *Proceedings of the SPIE Volume 7735*, ed. I. S. McLean, S. K. Ramsay, H. Takami, pp. 773524, (2010)
3. E. Diolaiti, J.-M. Conan, I. Foppiani et al., *Proceedings of the SPIE Volume 7736*, ed. B. L. Ellerbroek, M. Hart, N. Hubin, P. L. Wizinowich, pp. 77360R, (2010)
4. R. I. Davies, N. Ageorges, L. Barl et al., *Proceedings of the SPIE Volume 7735*, ed. I. S. McLean, S. K. Ramsay, H. Takami, pp. 77352A, (2010)

5. G. Herriot, D. Andersen, J. Atwood et al., *Proceedings of the 1st AO4ELT Conference - Adaptive Optics for Extremely Large Telescopes*, ed. Y. Clénet, J.-M. Conan, T. Fusco, G. Rousset, [02004], (2010)
6. J. M. Beckers, *Proceedings of the SPIE Volume 1114*, ed. F. J. Roddier, pp. 215 (1989)
7. E. Marchetti, R. Brast, B. Delabre et al., *Proceedings of the SPIE Volume 7015*, ed. N. Hubin, C. E. Max, P. L. Wizinowich, pp. 70150F, (2008)
8. B. Neichel, *This conference*, (2013)
9. F. Rigaut, *This conference*, (2013)
10. T. Pfrommer, P. Hickson, *JOSA A*, **27**, 11, pp. A97, (2010)
11. M. Lombini, G. Bregoli, G. Cosentino et al., *Proceedings of the SPIE Volume 7736*, ed. B. L. Ellerbroek, M. Hart, N. Hubin, P. L. Wizinowich, pp. 77365E, (2010)
12. L. Schreiber, M. Lombini, E. Diolaiti et al., *Proceedings of the SPIE Volume 7736*, ed. B. L. Ellerbroek, M. Hart, N. Hubin, P. L. Wizinowich, pp. 77365B, (2010)
13. M. Lombini, *This conference*, (2013)
14. N. Hubin, *This conference*, (2013)
15. P.-Y. Madec, *Proceedings of the SPIE Volume 8447*, ed. B. L. Ellerbroek, E. Marchetti, J.-P. Véran, pp. 844705, (2012)
16. J.-C. Siquin, J.-M. Lurçon, C. Guillemard et al., *Proceedings of the 1st AO4ELT Conference - Adaptive Optics for Extremely Large Telescopes*, ed. Y. Clénet, J.-M. Conan, T. Fusco, G. Rousset, [06004], (2010)
17. R. Biasi, D. Gallieni, P. Salinari et al., *Proceedings of the SPIE Volume 7736*, ed. B. L. Ellerbroek, M. Hart, N. Hubin, P. L. Wizinowich, pp. 77362B, (2010)